

General Disclaimer

One or more of the Following Statements may affect this Document

- This document has been reproduced from the best copy furnished by the organizational source. It is being released in the interest of making available as much information as possible.
- This document may contain data, which exceeds the sheet parameters. It was furnished in this condition by the organizational source and is the best copy available.
- This document may contain tone-on-tone or color graphs, charts and/or pictures, which have been reproduced in black and white.
- This document is paginated as submitted by the original source.
- Portions of this document are not fully legible due to the historical nature of some of the material. However, it is the best reproduction available from the original submission.



Technical Memorandum 82173

(NASA-TM-82173) ON SYNTHESSES OF THE X-RAY
BACKGROUND WITH POWER-LAW SOURCES (NASA)
22 p HC A02/NF A01 CSCL 03B

N85-12840

G3/90 Unclas
11494

On Syntheses of the X-ray Background with Power-Law Sources

G. DeZotti, E.A. Boldt, A. Cavaliere,
L. Danese, A. Franceschini, F.E. Marshall,
J.H. Swank, A.E. Szymkowiak

AUGUST 1981



National Aeronautics and
Space Administration

Goddard Space Flight Center
Greenbelt, Maryland 20771

On Syntheses of the X-ray Background with Power-Law Sources

G. De Zotti^{5,4}, E.A. Boldt¹, A. Cavaliere², L. Danese^{3,4}, A. Franceschini⁴,
F.E. Marshall¹, J.H. Swank¹, A.E. Szymkowiak¹

¹Laboratory for High Energy Astrophysics, NASA/Goddard Space Flight Center,
Greenbelt, Maryland 20771

²Istituto Astronomico, Universita di Roma, and Laboratorio di Astrofisica
Spaziale, Frascati (Roma), Italy

³Osservatorio Astronomico, Padova, Italy

⁴Scuola Internazionale Superiore di Studi Avanzati, Trieste, Italy

⁵Unita di Ricerca di Padova del GNA-CNR, Padova, Italy

Address for correspondence: E. Boldt
Code 661
Laboratory for High Energy Astrophysics
NASA/Goddard Space Flight Center
Greenbelt, Maryland 20771 USA

ABSTRACT

We discuss if and under what conditions the combined emission from power-law sources can mimic the XRB spectrum in the range 3-50 keV measured with the A2 experiment on HEAO-1. We confirm that a good fit can be obtained, but the required spectral properties of component sources differ from those observed for local active galactic nuclei. Strong constraints are deduced for the low luminosity extension and for the evolution of such local objects. We show that any other class of sources significantly contributing to the X-ray background must be characterized by an energy spectral index $\gamma \lesssim 0.4$, the mean index of the XRB (3-15 keV), and must exhibit steeper spectra at somewhat higher energies.

Subject headings: galaxies: cluster of - radiation mechanisms -
X-rays: sources - X-rays: spectra

I. INTRODUCTION

Although almost every class of known extragalactic objects have been found to be X-ray emitters, it is still unclear whether their integrated emission can account for the full intensity of the X-ray background (XRB). For the 2-10 keV band the most recent estimates yield a $\sim 5\%$ contribution from clusters of galaxies (McKee et al. 1980; Hintzen et al. 1980; Piccinotti et al. 1981) and a contribution $\approx 20\%$ for active galactic nuclei (Piccinotti et al. 1981). Moreover consideration of the constraints set by the deep survey counts (Giacconi et al. 1979), by the fluctuation level (Schwartz 1980) and by the optical counts at faint magnitudes (Kron 1980; Bahcall and Soneira 1980) has led to the conclusion that the contribution from quasars can not exceed 50% (Cavaliere et al. 1981).

The 3-50 keV XRB spectrum is very accurately described by a 40 keV thermal bremsstrahlung model (Marshall et al. 1980). Known spectra of single discrete sources do not resemble that of the XRB. The X-ray emitting plasma in clusters of galaxies has in most cases a temperature $\lesssim 10$ keV (Mushotzky et al. 1978). Excluding BL Lac type objects, the 3-50 keV spectra of a sample of 18 local active galaxies are power laws with energy index $\bar{\gamma}$ very close to 0.7 (Boldt 1980) and no evidence of steepening of the spectrum up to at least 80 keV has been found in the 8 objects for which higher energy measurements have been obtained (Mushotzky 1980, private communication). As for quasars, our spectral knowledge is limited to only two objects; although a thermal component compatible with the XRB is permitted for 3C273 (Worrall et al. 1977), radio quiet QSO 0241+622 requires $\gamma > 0.7$ (Worrall et al. 1980).

In order to account for the full XRB intensity either some superposition of suitably evolving active galactic nuclei or a new astrophysical component is apparently needed. While severe constraints are dictated by source counts

and by the fluctuation level, complementary information and additional constraints come from the observations of the XRB spectrum. A preliminary discussion, based on pre-HEAO-1 data, of the necessary conditions for the combined emission of non-thermal sources to mimic the observed spectral shape from 2 to 400 keV was carried out by Cavaliere et al. (1979, Paper I). This analysis was preliminary in that it was necessary to combine the existing measurements from basically different experiments so that systematic errors dominated the results: this fact was made apparent by the large values of χ^2 (> 2.7 per degree of freedom) which were obtained in any case (including thermal bremsstrahlung).

The A2 experiment on HEAO-1 has now provided a homogeneous set of high precision measurements, though covering a more limited energy range (3-50 keV). We present here a new analysis of the constraints set by such data on spectral properties of power-law sources that in principle could make up the XRB.

II. CLASSES OF MODELS

The guidelines for the choice of the empirical classes of power-law spectral models to be explored are supplied by an inspection of the observed XRB spectrum, which suggests the following strategy:

- (i) The bright resolved sources may (in fact, they likely do) dominate the XRB only at energies $\gtrsim 100$ keV (Boidt 1981). Progressively fainter and more numerous sources are required to make up the XRB at progressively lower energies; but then the component spectra should steepen or cut-off at characteristic energies $\bar{E} \lesssim 20(1+z)$ keV to conform to the steepening of the XRB spectrum at ≈ 20 keV.
- (ii) As this steepening appears now a gradual one with the present, sharply defined data, component spectra with a finite cut-off distribution are

required to successfully describe the smooth transition across 20 keV (note the variance with the pre-HEAO-1 notion of a sharp break in the XRB spectrum that required sharp and fixed cut-offs of the component spectra). This requirement can be relaxed if \bar{E} corresponds instead to a spectral break that is less drastic than a sharp cut-off.

Only two main classes of non-thermal sources comply with the above criteria (cf. Paper 1):

1) Sources whose power-law spectrum steepens at some energy E_b :

$$\lambda(E) = \lambda_0 \begin{cases} E^{-\gamma_1} & E \leq E_b \\ E_b^{\gamma_2 - \gamma_1} E^{-\gamma_2} & E > E_b \end{cases} \quad (1)$$

2) Sources having a power-law spectrum with a sharp cut-off at an energy E_c :

$$\lambda(E) = \begin{cases} \lambda_0 E^{-\gamma} & E \leq E_c \\ 0 & E > E_c \end{cases} \quad (2)$$

In order to reproduce the XRB spectrum with Model 2 a broad distribution of cut-off energies must also be assumed. Two possibilities have been considered:

2a) E_c evolves with redshift from the local observed values

$E_{c0} \sim$ some 10^2 keV obeying

$$E_c = E_{c0} (1+z)^{-\eta} \quad (3)$$

2b) the sources have, at any z , a power law distribution of cut-offs:

$$g(E_c) = \frac{1-\nu}{E_{cmax}^{1-\nu} - E_{cmin}^{1-\nu}} E_c^{-\nu} . \quad (4)$$

In all cases a number/luminosity evolution $\propto(1+z)^\alpha$ was allowed for.

The possibility that the XRB is saturated by an extrapolation at the faint end of the luminosity function of active galactic nuclei, without evolution, was also considered in Paper I. This possibility will not be discussed further here (except for a remark in Sect. 4) since it appears to be inconsistent with the flat faint end of that luminosity function as recently determined by Piccinotti et al. (1981).

As in Paper I, we allow for a gaussian distribution of spectral indices with mean values γ , γ_1 , and γ_2 and dispersions σ , σ_1 , and σ_2 respectively. We have neglected, however, the dispersion of E_b (model 1) or of E_{c0} (model 2a); this allows us to obtain (see Appendix), at least in the two cases $\Omega=1$ and $\Omega=0$ (Ω being the density parameter), explicit analytic expressions for the combined emission $I(E)$ of sources and therefore to keep within reasonable limits the computer time needed for the subsequent analysis.

III. RESULTS

As in Paper I we have applied the minimum χ^2 technique (see e.g. Avni 1976; Cash 1976) to determine the best fit values and the allowed ranges for the parameters. Minimizations have been carried out by the MINUITS CERN subroutine package, written by James and Roos.

The present analysis confirms the result of Paper I, that a suitable superposition of power law sources can represent the XRB spectrum as accurately as a thermal bremsstrahlung distribution. This is illustrated in Figs. 1 and 2, where the counts expected by convolving the spectrum predicted by Model 2a with the response functions of two detectors are compared with the observed ones. Table 1 gives, for all available data sets, the minimum values χ_{\min}^2 of χ^2 , the numbers of degrees of freedom ν and $\chi_{\nu}^2 = \chi_{\min}^2 / \nu$ associated with both power law and thermal bremsstrahlung models. Since the spread in the results from different detector layers exceeds that expected from counting statistics alone, in computing these values a 2% contribution of systematic errors to the overall uncertainty has been allowed for. We have not distinguished between power law models 1, 2a and 2b since the corresponding χ_{\min}^2 do not differ significantly. While it is possible to fit the HEAO-1 data with these models, the fits are much more tightly restricted than they were by the composite data used for Paper I. It is thus more significant that fits can be obtained.

For the low energy slope and its dispersion the results of fitting the HEAO-1 data differ from the best fit results in Paper I, although they lie in the large possible ranges of parameters found there. No sign has been found in the HEAO-1 data of the slight flattening of the XRB spectrum from 3 to 15 keV which is to be expected in the presence of a large dispersion in the spectral indices of contributing sources (the slope of $I(E)$ is given by $-\gamma + \frac{1}{2} \sigma^2 \ln E / 2\sqrt{5}$, cfr. eqs. (A1)-(A4)) and which seemed to be born out by pre-HEAO-1 data (cfr. Fig. 1 in Paper I). The HEAO-1 data require that the dominant contributors to the XRB have a rather narrow range of spectral indices centered around $\gamma \approx 0.4 \pm 0.5$. This point is specified in Fig. 3 which shows the 90% confidence contours for γ (or γ_1) and σ (or σ_1) following from

both HED1 and HED3 combined layers data (these contours are essentially identical for all models considered here). As expected, the constraints on the slope γ_2 of Model 1 are not so sharply defined. Our spectral fits indicate $1.2 < \gamma_2 < 1.4$ with $\sigma_2 < 0.35$.

The other important parameter for comparison with direct observations is the energy \bar{E} at which the spectral break or the cut-off occurs. For model 1 we find a best fit value $E_b = 50-55$ keV (the exact value being slightly different when data from different detectors are used) with an allowed range (90% confidence) 40-60 keV. As for model 2a, the limited energy range covered by HEAO-1 data does not allow a precise definition of E_{CO} . The formal best fit value is $E_{CO} = 500$ keV with a 90% confidence lower limit $E_{CO} > 300$ keV; the upper limit is undetermined. The value of η is strongly correlated with the value of E_{CO} (it increases with E_{CO} following the approximate relationship given by Eq. (6) of Paper I): we have $\eta \approx 1.4$ if $E_{CO} = 500$ keV, $\eta \approx 1.1$ for $E_{CO} \approx 300$ keV, and $\eta \approx 2.25$ for $E_{CO} \approx 1500$ keV.

The quality of the fit turns out to be rather insensitive to the assumed value of α (i.e. to the rate of evolution) as far as models 1 and 2b are concerned; in both cases however values of $\alpha > 3$ are favoured, lower values producing an insufficient bending down of $I(E)$ because of the smearing out effect of the redshift distribution. For the same reason we expect, especially in the case of model 1, that a stronger evolution be associated with spectra having a round knee instead of a cut-off or a sharp break. On the other hand, for model 2a the rate of evolution plays a direct role in the definition of the effective distribution of cut-off energies, see Eq. (3); only with $3.5 < \alpha < 5$ can a good fit be obtained.

IV. DISCUSSION

If the XRB spectrum is to be interpreted in terms of emission from

unresolved sources, its remarkable smoothness in the 3-50 keV range seems to demand that most of the observed intensity comes from a single, fairly homogeneous population with a mean spectral index γ_1 (or γ) definitely flatter than that of local AGN's, and with a cut-off or a break occurring at relatively low energies, again at variance with the (however limited) observations of local AGN's. These two facts pose serious difficulties to all attempts at relating the main contributors to the XRB with local AGN's. For example, although model 2a incorporates the large values of E_{c0} suggested by the presently available observations, it is constrained by the observed local luminosity function for AGN's and requires an evolution in number/luminosity associated with a downward evolution of E_c . Furthermore, to recover an effective distribution function of γ 's sharply peaked around $\bar{\gamma}=0.4$, the spectral index of the XRB from 3 to 15 keV, the spectral indices of the sources must also evolve (i.e. they must, on the average, decrease with z increasing) and such evolution must be much faster than that of E_c . For example, an exponential evolution of γ ($\gamma=\gamma_0 \exp[-q]1-t/t_0$) with $\gamma_0 = 0.7$ and $q = 1.3+1.4$ coupled with an exponential luminosity evolution ($L=L_0 \exp[Q(1-t/t_0)]$) with $Q = 4$ seems to be needed to obtain a good fit of the < 15 keV XRB spectrum; but an exponential luminosity evolution also results in an effective distribution of E_c which is not broad enough to avoid a steep decline of the computed XRB spectrum at $E > 15$ keV, for any value of η (cf. eq. (3)).

In the case of models 1 and 2b, continuity with local AGN's is not required (and forcing such a continuity would anyway bring in the previously noted difficulties). On the other hand, if the main contributors to the XRB are unrelated to AGN's the possible contribution to the XRB of the AGN's themselves must be $< 30\%$, because a larger contribution from objects

with $\gamma=0.7$ would prejudice any fit. This limit is the most stringent to date; it implies both that the luminosity function of AGN's with $\gamma=0.7$ must converge not far below $L(2-10) \text{ keV} \approx 10^{42} \text{ erg/s}$, and that essentially no evolution of these objects is allowed, in X-rays at least. The only possibility for a downward extension of the AGN luminosity function would imply a γ abruptly switching to a value ≈ 0.4 at $L \approx 10^{42} \text{ erg/s}$.

Indeed, the spectral properties of any population of power-law sources significantly contributing to the XRB intensity are severely constrained. Since the allowed dispersion of spectral indices $\sigma_{\gamma} < 0.2$ is already almost completely saturated by AGN's, any other population must be γ (or γ_1) $\lesssim 0.4$, the mean spectral index of the XRB in the range 3-15 keV. This implies, for example, that QSO's either have the same spectral index as the yet unknown population which saturates the XRB intensity, or have a steep spectrum and make only a small contribution to the XRB above 3 keV.

Similar considerations would constrain the evolutionary properties of sources (such as BL Lac's) having a very flat ($\gamma=0$) spectral index well above 3 keV. On the other hand, the spectra of BL Lac type objects tend to be relatively steep at $\lesssim 3 \text{ keV}$ (Holt 1980) indicating that their contribution to the XRB could be substantial only for the soft part of the spectrum that is still not well defined.

ACKNOWLEDGMENTS

We are indebted to R. Shafer for assistance in the computer programming and for useful discussions. We are also grateful to S. Holt and R. Mushotzky for useful discussions. G.D.Z. wishes to thank the GSFC X-ray Astronomy group and the University of Maryland for their hospitality. A.C., L.D., G.D.Z. and A.F. acknowledge funding by National Research Council (CNR) of Italy.

Appendix

The relevant formulae for computing the combined emissions of power law sources are given in the Appendix of Paper I to which the reader is also referred for nomenclature. Neglecting the dispersion of the break and cut-off energies (i.e. setting $g(E_{b(c)}) = \delta(E'_{b(c)} - E_{b(c)})$ and replacing $(1+z)$ with its weighted average $(1+z_{1(2)})$ in the expressions $0.5 \sigma^2 \ln(1+z)$ (and in the analogous ones with σ_1^2 and σ_2^2) we obtain the results listed below for the various models. We have checked that the above mentioned approximation introduces an error smaller than 1% for the interesting values of σ 's ($\sigma < 0.5$).

For model 1 the integrated emission reads:

$$\begin{aligned}
 I(E) = K & \left(\frac{E}{2\sqrt{5}} \right)^{-\gamma_1 + \frac{1}{2} \sigma_1^2 \ln(E/2\sqrt{5})} \cdot \frac{(1+z_M)^{\zeta_1+1} - (1+z_m)^{\zeta_1+1}}{1+\zeta_1} + \\
 & + \left(\frac{E_b}{2\sqrt{5}} \right)^{-\gamma_1 + \frac{1}{2} \sigma_1^2 \ln\left(\frac{E_b}{2\sqrt{5}}\right)} \left(\frac{E}{E_b} \right)^{-\gamma_2 + \frac{1}{2} \sigma_2^2 \ln(E/E_b)} \cdot \frac{(1+z_M)^{\zeta_2+1} - (1+z_m)^{\zeta_2+1}}{1+\zeta_2} \quad (A1)
 \end{aligned}$$

where

$$K = \frac{c}{4\pi H_0} \frac{N_0 \bar{L}}{2\sqrt{5} \ln 5} \quad (A2)$$

and

$$\zeta_1 = \alpha - 2 - \omega + \gamma_1 + \frac{1}{2} \sigma_1^2 \ln \left[\left(\frac{E}{2\sqrt{5}} \right)^2 (1+z_1) \right]$$

$$\zeta_2 = \alpha - 2 - \omega - \gamma_2 + \frac{1}{2} \sigma_2^2 \ln \left[\left(\frac{E}{E_b} \right)^2 (1+z_2) \right]$$

$$z_m = \text{Max} [0, E_b/E - 1]$$

$$z_M = \text{Min} [z_{\text{max}}, E_b/E - 1] .$$

In actual calculations $\omega=0.5$ (corresponding to $\Omega=1$; see eq. (5) of Paper I) and $z_{\text{max}}=3$ have been adopted. The normalization energy $2\sqrt{5}$ keV is fixed by our assumption of a 2-10 keV luminosity function independent of the spectral index.

For model 2a the result is:

$$I(E) = K \left(\frac{E}{2\sqrt{5}} \right)^{-\gamma + \frac{1}{2} \sigma^2 \ln(E/2\sqrt{5})} \cdot \frac{(1+z_M)^{\delta+1} - 1}{\delta+1} \quad (\text{A3})$$

$$z_M = \text{Min} [z_{\text{max}}, (E_{\text{co}}/E)^{1/(1+\eta)} - 1]$$

$$\delta = \alpha - 2 - \omega - \gamma + \frac{1}{2} \sigma^2 \ln \left[\left(\frac{E}{2\sqrt{5}} \right)^2 (1+z_1) \right] .$$

Finally for model 2b we have:

$$I(E) = K \left(\frac{E}{2\sqrt{5}} \right)^{-\gamma + \frac{1}{2} \sigma^2 \ln(E/2\sqrt{5})} J(E) \quad (\text{A4})$$

with

$$J(E) = \frac{(1+z_M)^{\delta+1} - 1}{\delta+1} \quad \text{for } E \leq E_{\text{cmin}}/(1+z_M)$$

$$J(E) = \frac{(E_{\text{cmin}}/E)^{\delta+1} - 1}{\delta+1} + \frac{1}{E_{\text{cmax}}^{1-\nu} - E_{\text{cmin}}^{1-\nu}} \left\{ E_{\text{cmax}}^{1-\nu} \frac{(1+z_M)^{\delta+1} - (E_{\text{cmin}}/E)^{\delta+1}}{\delta+1} - \right.$$

$$\left. - E^{1-\nu} \frac{(1+z_{\text{max}})^{\delta+2-\nu} - (E_{\text{cmin}}/E)^{\delta+2-\nu}}{\delta+2-\nu} \right\} \quad \text{for } \frac{E_{\text{cmin}}}{1+z_M} < E < E_{\text{cmin}}$$

$$J(E) = \frac{1}{E_{\text{cmax}}^{1-\nu} - E_{\text{cmin}}^{1-\nu}} \left\{ E_{\text{cmax}}^{1-\nu} \frac{(1+z_M)^{\delta+1} - 1}{\delta+1} - E^{1-\nu} \frac{(1+z_M)^{\delta+2-\nu} - 1}{\delta+2-\nu} \right\}$$

for $E > E_{\text{cmin}}$

$$z_M = \text{Min} (z_{\text{max}}, E_{\text{cmax}}/E - 1) ,$$

δ is the same as for the model 2a.

ORIGINAL PAGE IS
OF POOR QUALITY

REFERENCES

- Avni, Y. 1976, Ap. J. 210, 642.
- Bahcall, J.N., and Soneira, R.M. 1980, Ap. J. (Letters) 238, L17.
- Boldt, E.A. 1981, Proceedings of Uhuru Memorial Symposium; Journal Washington Academy Science, in press.
- Boldt, E.A. 1981, Comments on Astrophysics 9, 97.
- Cavaliere, A., Danese, L., De Zotti, G., and Franceschini, A. 1979, Astr. Ap. 79, 169 (Paper I).
- Cavaliere, A., Danese, L., De Zotti, G., and Franceschini, A. 1981, Astr. Ap. 97, 269.
- Cash, W. 1976, Astr. Ap. 52, 307.
- Giacconi, R. et al. 1979, Ap. J. (Letters) 234, L1.
- Hintzen, P., Scott, J.S., and McKee, J.D. 1980, Ap. J. 242, 857.
- Holt, S.S. 1980, NASA TM 82010.
- Kron, R. 1980, in ESO Workshop in Two-Dimensional Photometry, P.O. Linblad and H. van der Laan eds., Geneva.
- Marshall, F.E., Boldt, E.A., Holt, S.S., Miller, R.B., Mushotzky, R.F., Rose, L.A., Rothschild, R.E., and Serlemitsos, P.J. 1980, Ap. J. 235, 4.
- McKee, J.D., Mushotzky, R.F., Boldt, E.A., Holt, S.S., Marshall, F.E., Pravdo, S.H., and Serlemitsos, P.J. 1980, Ap. J. 242, 843.
- Mushotzky, R.F., Serlemitsos, P.J., Smith, B.W., Boldt, E.A., and Holt, S.S. 1978, Ap. J. 225, 21.
- Piccinotti, G., Mushotzky, R.F., Boldt, E.A., Holt, S.S., Marshall, F.E., and Serlemitsos, P.J. 1981, Ap. J., in press.

Schwartz, D.A. 1980, *Physica Scripta* 21, 644.

Worrall, D.M., Mushotzky, R.F., Boldt, E.A., Holt, S.S., and Serlemitsos, P.J.
1979, *Ap. J.* 232, 683.

Worrall, D.M., Boldt, E.A., Holt, S.S., and Serlemitsos, P.J. 1980, *Ap. J.*
240, 421.

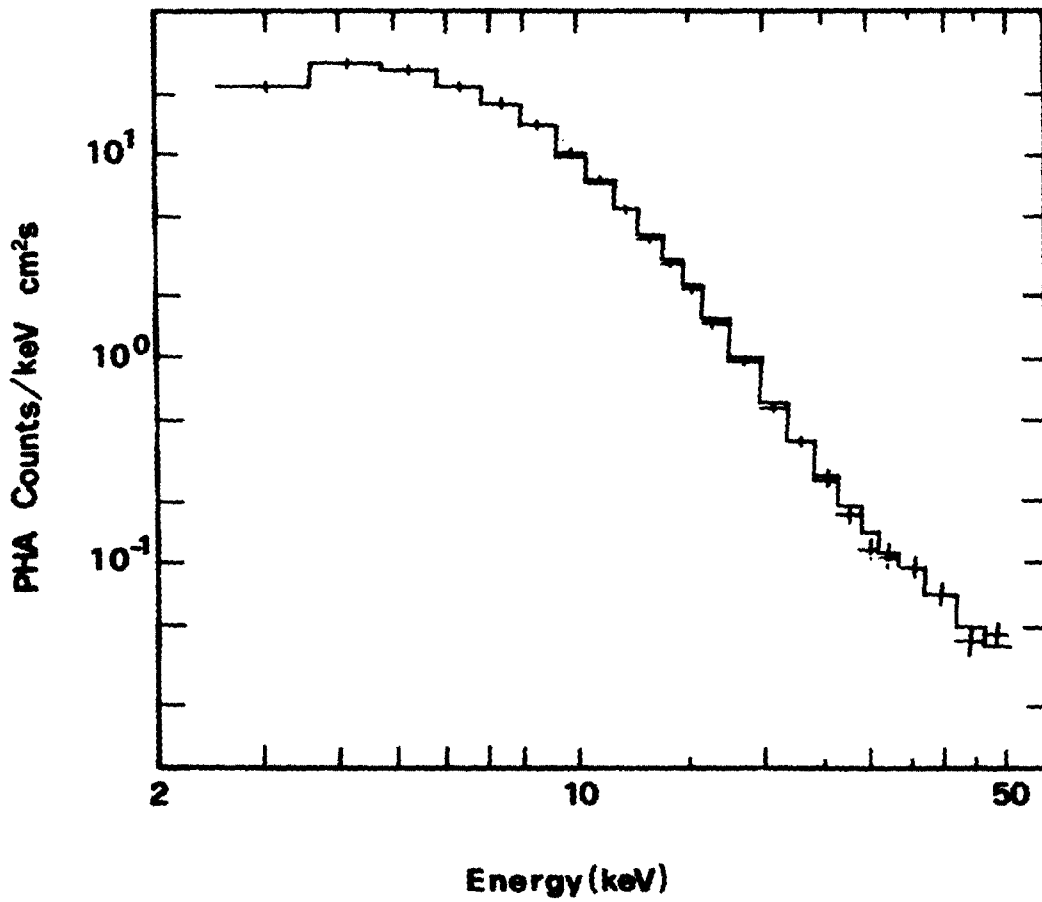
Table 1

Detector	Power law			Thermal bremsstrahlung		
	χ^2_{\min}	ν	χ^2_{ν}	χ^2_{\min}	ν	χ^2_{ν}
HED 1						
Layer 1	22	17	1.3	24	21	1.1
Layer 2	23	12	1.9	30	15	2.0
Combined Layers	33	17	1.9	23	21	1.1
HED 3						
Layer 1	24	17	1.4	30	21	1.9
Layer 2	11	12	0.90	12	15	0.8
Combined Layers	14	17	0.85	20	21	1.0
MED 1						
Layer 1	19	19	1.0			

Figure Captions

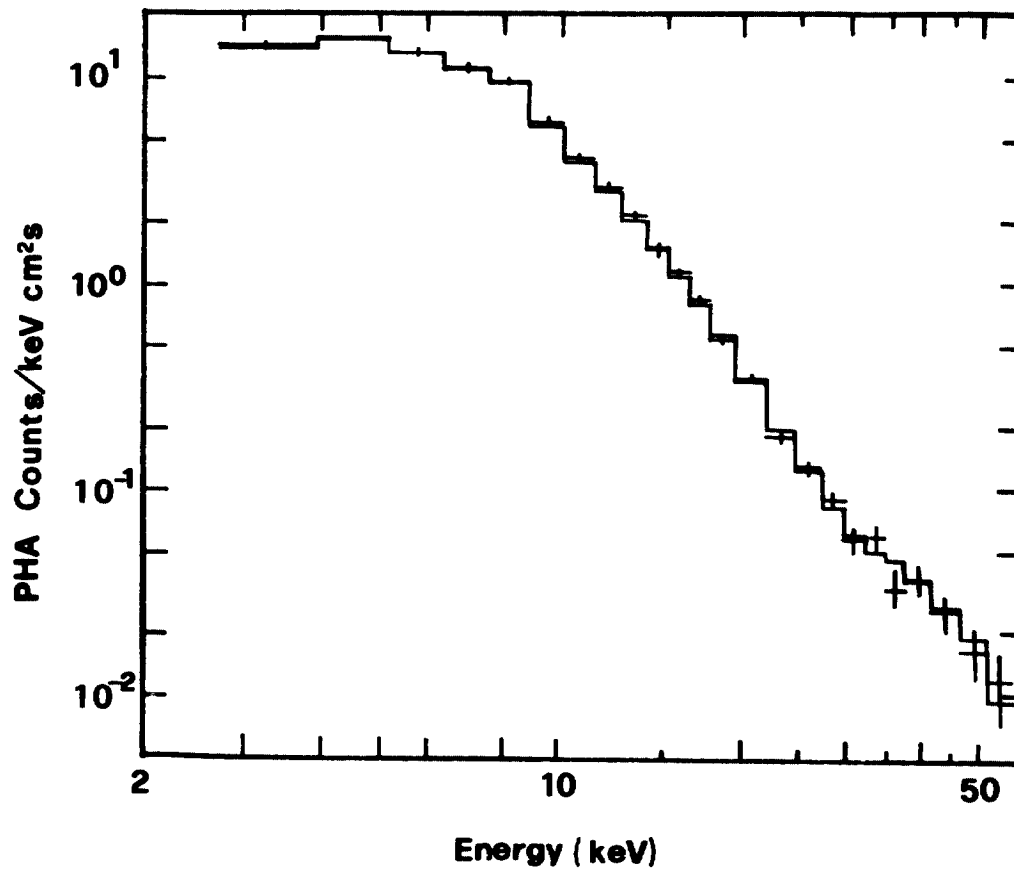
- Fig. 1 - Comparison of the counts from layer 1 of HED 1 with those predicted by Model 1a with $\alpha=4.0$, $\gamma=0.465$, $\sigma=0.065$, $E_{co}=400$ keV, $\eta=1.35$.
- Fig. 2 - Comparison of the counts from layer 1 of HED 3 with those predicted by Model 2a with the same values of the parameters as for Fig. 1 except for $\eta=1.25$.
- Fig. 3 - Constant χ^2 contours at $\chi^2=\chi_{min}^2+4.6$ in the γ - σ plane for HED 1 (continuous line) and HED3(dashed line) combined layers data. If we do not care about the values of all other parameters, these contours bound the 90% confidence region for γ and σ . The best fit values of the parameters corresponding to HED 1 combined layers (\odot), HED 3 combined layers (\otimes) and MED layer 1 (\oplus) are also shown. Model 2a.

FIG.1



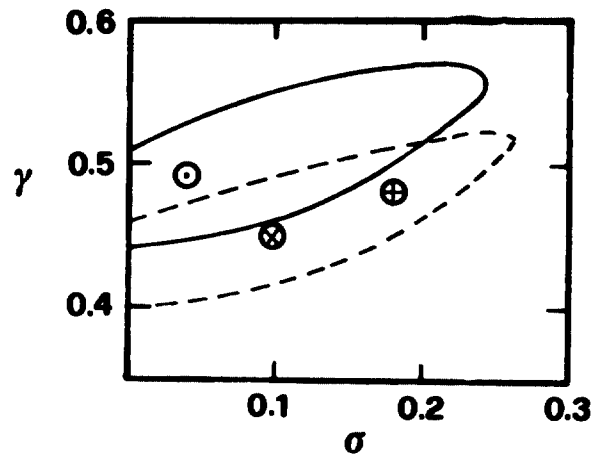
ORIGINAL PAGE IS
OF POOR QUALITY

FIG. 2



ORIGINAL PAGE IS
OF POOR QUALITY

FIG. 3



ORIGINAL PAGE IS
OF POOR QUALITY

E.A. BOLDT, F.E. MARSHALL, J.H. SWANK, and A.E. SZYMKOWIAK:

Code 661, Laboratory for High Energy Astrophysics,

NASA Goddard Space Flight Center, Greenbelt, MD 20771

A. CAVALIERE: Istituto Astronomico, Università di Roma,

Piazzale A. Moro, 2, I-00185 Roma, Italy

L. DANESE, and G. DE ZOTTI: Istituto di Astronomia, Vicolo dell'Os

servatorio 5, I-35100 Padova, Italy

A. FRANCESCHINI: Scuola Internazionale Superiore di Studi Avanzati,

Strada Costiera 11, I-34014 Trieste, Italy